Oligomer Formation of Toxic and Functional Amyloid Peptides Studied with Atomistic Simulations

ARTICLE *in* THE JOURNAL OF PHYSICAL CHEMISTRY B · JUNE 2015

Impact Factor: 3.3 · DOI: 10.1021/acs.jpcb.5b04822 · Source: PubMed

3 AUTHORS, INCLUDING:

Ahmed E. Ismail
West Virginia University
66 PUBLICATIONS **491** CITATIONS
SEE PROFILE

Birgit Strodel
Forschungszentrum Jülich
43 PUBLICATIONS **479** CITATIONS
SEE PROFILE

THE JOURNAL OF PHYSICAL CHEMISTRY B

Article

pubs.acs.org/JPCB

Oligomer Formation of Toxic and Functional Amyloid Peptides Studied with Atomistic Simulations

Martín Carballo-Pacheco,[†,‡] Ahmed E. Ismail,[†] and Birgit Strodel*[,‡,¶]

[†]AICES Graduate School and Aachener Verfahrenstechnik: Molecular Simulations and Transformations, RWTH Aachen University, Schinkelstraße 2, 52062 Aachen, Germany

[‡]Institute of Complex Systems: Structural Biochemistry (ICS-6), Forschungszentrum Jülich GmbH, 52425 Jülich, Germany

[¶]Institute of Theoretical and Computational Chemistry, Heinrich Heine University Düsseldorf, Universitätstraße 1, 40225 Düsseldorf, Germany

Supporting Information

ABSTRACT: Amyloids are associated with diseases, including Alzheimer's, as well as functional roles such as storage of peptide hormones. It is still unclear what differences exist between aberrant and functional amyloids. However, it is known that soluble oligomers formed during amyloid aggregation are more toxic than the final fibrils. Here, we perform molecular dynamics simulations to study the aggregation of the amyloid-β peptide Aβ_{25-35}, associated with Alzheimer's disease, and two functional amyloid-forming tachykinin peptides: kassinin and neuromedin K. Although the three peptides have similar primary sequences, tachykinin peptides, in contrast to Aβ_{25-35}, form nontoxic amyloids. Our simulations reveal that the charge of the C-terminus is essential to controlling the aggregation process. In particular, when the kassinin C-terminus is not amidated, the aggregation kinetics decreases considerably. In addition, we observe that the monomeric peptides in extended conformations aggregate faster than those in collapsed hairpin-like conformations.

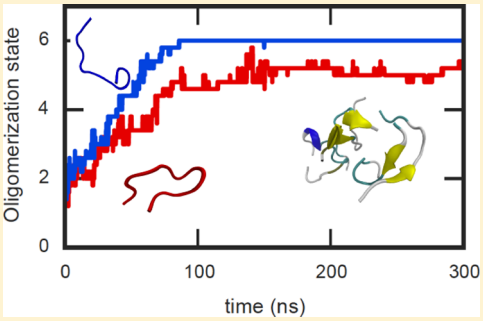

INTRODUCTION

Amyloids are highly structured protein aggregates. These aggregates form long fibrils with a cross-β sheet structure, in which proteins lie perpendicular to the fibril axis in a β-sheet conformation. Amyloids have been studied at length because of their implication in diseases such as Alzheimer's disease, Parkinson's disease, and type II diabetes.[1,2] However, it is still unclear what role amyloids play in these diseases. Recent experimental evidence shows that transient oligomers, rather than large structured fibrils, are more toxic.[3−6] The reason for this toxicity also remains under debate, although experimental results suggest that the cytotoxicity is due to oligomers disrupting cell membranes.[7,8] Interaction with membrane-associated protein receptors is also considered as a possible reason for the toxicity of oligomers.[9]

While most amyloids are associated with diseases, an increasing number of amyloids, called functional amyloids, have been found to have physiologically normal functions,[1,10,11] such as storage of peptide hormones,[12] acting as scaffolds in melanin formation[13] and signaling complexes in programmed necrosis.[14] The discovery of functional amyloids has changed our understanding of the amyloid fold. Since most amyloids have been associated with diseases, it was assumed that they are inherently toxic. However, functional amyloids must have had evolutionary pressure to reduce their toxicity. It has been suggested that, unlike aberrant amyloids, functional amyloids grow in a highly regulated environment that limits their toxicity.[12] It has also been observed that some functional amyloids, e.g., Pmel17, form fibrils faster than aberrant amyloids,[13] with a very short toxic oligomer phase before rapidly entering into the nontoxic fibril phase.

Of the various known functional amyloids, a number of peptide hormones stored as amyloids in pituitary secretory granules have received much attention. Maji et al.[12] first noted that these peptides are stored as amyloids and are later released into the extracellular space, where they dissolve into monomers and function as hormones. Among these peptides, tachykinin peptides, such as neuromedin K (also called neurokinin B)[12] and kassinin,[15] are of particular interest. Tachykinin peptides are a family of neuropeptides that are found in animals ranging from amphibians to mammals and which have disparate functions such as exciting neurons, contracting muscles, and dilating blood vessels.[16] Tachykinin peptides share a common C-terminus: -Phe-X-Gly-Leu-Met-NH_2, where X is an aromatic or aliphatic residue.[16] This C-terminus is remarkably similar to the C-terminus of the fraction 25 to 35 of the amyloid-β peptide (Aβ), which plays a key role in the development of Alzheimer's disease. Moreover, tachykinin peptides can coaggregate with Aβ[17] and decrease its toxicity.[18] Aβ_{25-35} has been shown to aggregate[19,20] and to be neurotoxic[21,22] on its

Received: May 20, 2015
Revised: June 29, 2015
Published: June 30, 2015

DOI: 10.1021/acs.jpcb.5b04822
J. Phys. Chem. B 2015, 119, 9696−9705

own, and it is thus used as a representative of the full-length Aβ peptide.[20,23] Although tachykinin peptides share certain sequence similarity with $A\beta_{25-35}$ (see Table 1) and aggregate into amyloid fibrils, these aggregates are not toxic.[15] It should be noted, though, that tachykinin peptides have an amidated C-terminus,[16] while $A\beta_{25-35}$ is usually studied with a free acid C-terminus.[20,22−24] It has been observed that when the C-terminus of $A\beta_{25-35}$ is amidated its toxicity decreases drastically.[22] Understanding why peptides with such similar sequences behave so differently is essential to elucidate the difference in aggregation between functional and aberrant amyloids.

Table 1. Primary Structure of the Peptides under Study[a]

peptide	sequence
$A\beta_{25-35}$	H-GSNKGAIIGLM-OH
kassinin	H-DVPKSDQFVGLM-NH_2
neuromedin K	H-DMHDFFVGLM-NH_2

[a]Kassinin and neuromedin K are part of the tachykinin peptide family.

Although amyloids have been studied at length, it is still unclear what intrinsic or environmental factors affect protein aggregation. Intrinsic factors are characteristics of polypeptide chains; peptides that aggregate tend to have high hydrophobicity,[25] low charge,[25] a large number of alternating hydrophobic−hydrophilic residues,[25] and high β-sheet propensity.[26] Some environmental factors that influence amyloid aggregation are pH,[27] temperature,[28] salt ions and ionic strength,[29−31] hydrostatic pressure[32] and the presence of crowding agents.[33] Even though there is now a wealth of information on the influence of determinants on fibril growth,[25,26,28−32] little is known about their influence on the aggregation kinetics and conformations of oligomers.

Since oligomers are the most toxic species of aberrant amyloids, it would be of interest to observe if there are differences between the early aggregates of tachykinin peptides and $A\beta_{25-35}$ and the influence of aggregation determinants on these oligomers. Because of their transient existence it is hard to study and characterize these aggregates experimentally. In such cases, atomistic molecular dynamics (MD) simulations can provide mechanistic details and complement indirect experimental evidence.[34−37] In particular, atomistic MD simulations have already been used to understand the formation of amyloid oligomers of GNNQQNY from Sup35,[38−40] sections of the tau protein, β_2 microglobulin,[41] insulin,[42] and α-synuclein,[43−45] sections of Aβ,[40,46−50] and full-length Aβ.[51]

In this paper, we present simulations of the initial aggregation of two tachykinin peptides (kassinin and neuromedin K) and $A\beta_{25-35}$, with amidated and free acid C-termini and at different salt concentrations. All-atom, explicit-solvent simulations were performed, in which six monomers were freely allowed to aggregate. We observe that tachykinin peptides aggregate faster than $A\beta_{25-35}$, and that peptides with an extended conformation aggregate faster than those which have a hairpin-like conformation.

METHODS

Simulated Systems. To study the aggregation of $A\beta_{25-35}$, kassinin, and neuromedin K, six monomers of each peptide were randomly placed in cubic boxes at a concentration of 10 mM. Six peptides were chosen to balance the competing goals of keeping the peptide concentration low enough to allow monomers and oligomers to change conformations between collisions and keeping the overall system size manageable. Table 2 provides a summary of the simulations performed in this work. Five replicates of each system were simulated for 300 ns each to minimize statistical errors arising from stochasticity in the aggregation process. Each peptide was studied at concentrations of 0 and 150 mM NaCl. Systems at 0 mM salt concentration were simulated with enough counterions to neutralize the system. $A\beta_{25-35}$ and kassinin were studied both with free acid and amidated C-termini. Finally, $A\beta_{25-35}$ was studied in a restrained hairpin-like conformation as explained in the next section. One simulation for each peptide at 0 mM salt concentration was extended to 1 μs to test how the initially formed oligomers evolve. A total of 30 μs were simulated. Each system contained around 130,000 atoms. Neuromedin K was simulated with protonated His^3. To test the influence of the protonation state of His^3, the simulation at 0 mM NaCl was repeated with unprotonated His^3 (protonated only at N_ϵ); the effect is negligible (Figure S1, Supporting Information).

Table 2. Summary of Performed Aggregation Simulations

peptide	N-terminus	C-terminus	NaCl (mM)	time (ns/run)	no. of simulations
$A\beta_{25-35}$	$-NH_3^+$	$-COO^-$	0	300	4
				1000	1
kassinin	$-NH_3^+$	$-CONH_2$	0	300	4
				1000	1
neuromedin K	$-NH_3^+$	$-CONH_2$	0	300	4
				1000	1
$A\beta_{25-35}$	$-NH_3^+$	$-CONH_2$	0	300	5
kassinin	$-NH_3^+$	$-COO^-$	0	300	5
restrained $A\beta_{25-35}$	$-NH_3^+$	$-COO^-$	0	300	5
kassinin in a β-hairpin	$-NH_3^+$	$-CONH_2$	0	300	5
$A\beta_{25-35}$	$-NH_3^+$	$-COO^-$	150	300	5
kassinin	$-NH_3^+$	$-CONH_2$	150	300	5
neuromedin K	$-NH_3^+$	$-CONH_2$	150	300	5

Simulation Setup and Parameters. All simulations were performed using the GROMACS software package (version 4.6),[52] with the OPLS-AA force field[53,54] and the TIP4P water model.[55] Structures were visualized using VMD.[56]

The starting conformation for the aggregation simulations were obtained from a simulation of the monomer of each system. The monomer simulations of $A\beta_{25-35}$, kassinin and neuromedin K were started from the structures with Protein Database codes 1QYT (model 1),[24] 1MYU,[57] and 1P9F,[58] respectively. The monomers were placed in a periodic cubic box sufficiently large so that the walls were at least 1.2 nm away from the peptide. Counterions were added to neutralize the system. Further salt was added to obtain the desired salt concentration (see Table 2). The systems were minimized with the steepest descent algorithm, followed by equilibrations via a 100 ps *NVT* simulation and subsequently a 100 ps *NPT* simulation. During the equilibration, the protein backbone was restrained. Finally, a 50 ns *NPT* simulation was performed for each system. In this manner, the initial experimental helical conformations for each peptide, which were obtained in hydrophobic solvents, were disassembled and the peptides were mostly unstructured. These simulations were performed to create initial configurations for the aggregation simulations.

DOI: 10.1021/acs.jpcb.5b04822
J. Phys. Chem. B 2015, 119, 9696−9705

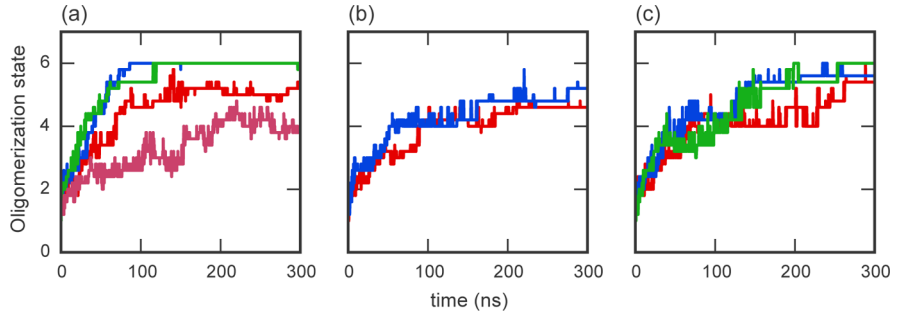

Figure 1. Oligomerization state as a function of simulation time for Aβ_{25-35} (red), kassinin (blue) and neuromedin K (green) in (a) 0 mM NaCl with standard termini, (b) 0 mM NaCl with nonstandard termini (i.e., amidated C-terminus for Aβ_{25-35} and free acid C-terminus for kassinin), and (c) 150 mM NaCl with standard termini. In plot (a), Aβ_{25-35} with a restrained hairpin-like conformation is also plotted in pink (bottom curve).

To study the aggregation of each peptide, six conformations were selected at random from the last 25 ns of each monomer simulation. When analyzing the aggregation simulations, we realized that the monomer conformations are relevant for the aggregation kinetics. Thus, we extended the monomer simulations to 1 μs. Because the conformation of the kassinin monomer changed dramatically in the 1 μs simulation, we repeated the aggregation simulation (called kassinin in a β-hairpin conformation in Table 2). In this case, monomers were selected at random from the last 800 ns of the 1 μs simulation. In all aggregation simulations, the six monomers were placed randomly in a periodic cubic box with 10 nm edge length, resulting in a concentration of ~10 mM. The systems were solvated and ions were added to neutralize the system and reach the desired salt concentration (see Table 2). The systems were equilibrated with a 1 ns *NVT* simulation and a 1 ns *NPT* simulation. During equilibration, the protein backbone was restrained. After equilibration, the proteins were allowed to move without restraints, with the exception of the simulation where Aβ_{25-35} was restrained in a hairpin-like conformation. In this simulation, a restraint was introduced between the side-chain nitrogen of Lys^4 and the carboxylic acid carbon of the C-terminus (for ease of comparison, residues in Aβ_{25-35} are counted starting from 1 instead of 25). The restraint was applied according to the following equation:

$$V(r_{ij}) = \begin{cases} \frac{1}{2}k(r_{ij} - r_0)^2, & r_{ij} < r_0, \\ 0, & r_0 \le r_{ij} < r_1, \\ \frac{1}{2}k(r_{ij} - r_1)^2, & r_1 \le r_{ij} < r_2, \\ \frac{1}{2}k(r_2 - r_1)(2r_{ij} - r_2 - r_1), & r_2 \le r_{ij}, \end{cases} \quad (1)$$

where r_{ij} is the distance between the aforementioned C and N atoms, r_0 = 0.2 nm, r_1 = 0.5 nm, r_2 = 0.6 nm and $k = 10^5$ kJ mol^{-1} nm^{-2}.

The following parameters were used for production runs. A cutoff of 1 nm was used for van der Waals interactions and short-range Coulombic interactions. Long-range electrostatic interactions were calculated every time step with the particle mesh Ewald method[59] using a grid spacing of 0.12 nm in conjunction with periodic boundary conditions. Peptide bonds were constrained with the P-Lincs algorithm[60] and water molecules were constrained with the SETTLE algorithm.[61] Virtual interaction sites were used for all hydrogens,[62] which permitted a 5 fs time step. Pressure was kept constant at 1 bar with the Parrinello−Rahman barostat[63,64] and temperature was kept constant at 310 K with the Nosé−Hoover thermostat.[65,66]

Analysis. Simulations were analyzed with help of the GROMACS software package tools[52] and the MDAnalysis package.[67] Two peptides *i* and *j* are considered to have aggregated if any atom of peptide *i* is within 0.5 nm of any atom of peptide *j*. For the aggregation kinetics plots (e.g., Figure 1), the average maximum oligomerization state is plotted. That is, the maximum oligomerization state is calculated for each simulation and then averaged over the five simulations of each system. For the oligomer contact maps, residues *i* and *j* are considered to be in contact when any atom of residue *i* is within 0.5 nm of any atom of residue *j*, where *i* and *j* are from different monomers. These contact maps include the information from all oligomers (i.e., dimers to hexamers) from the 300 ns aggregation simulations. The contact maps are later normalized by the number of possible contacts. For the monomer contact maps, residues *i* and *j* are considered in contact when any atom of residue *i* is within 0.4 nm of any atom of residue *j*. The solvent accessible surface area (SASA) for hydrophobic atoms is calculated using the algorithm of Eisenhaber et al.[68] as implemented in GROMACS,[52] where atoms with charge less than 0.2 are considered hydrophobic. The secondary structure was classified based on the DSSP algorithm.[69] To calculate how spherical an aggregate is, the asphericity was calculated[70] as

$$\Delta = \frac{3}{2}\frac{\sum_{i=1}^{3}(\lambda_i - \bar{\lambda})^2}{(\mathrm{tr}\,\mathbf{T})^2} \quad (2)$$

with

$$\bar{\lambda} = \frac{\mathrm{tr}\,\mathbf{T}}{3} \quad (3)$$

where $\mathbf{T}$ is the inertia tensor and λ_i are the eigenvalues of $\mathbf{T}$. Asphericity is defined as a number between 0 and 1; when Δ = 0, the protein is perfectly spherical; as Δ increases, the protein becomes more aspherical. To estimate the properties of hexamers, snapshots were taken every 500 ps and considered only when they were classified as hexamers as defined above. Monomers were clustered based on the root-mean-square deviation of the atomic positions using the algorithm from Daura et al.[71]

RESULTS

Aggregation of Tachykinin Peptides and Aβ_{25-35}. To study the aggregation of Aβ_{25-35}, kassinin and neuromedin K, five independent explicit-solvent atomistic MD simulations were performed for each system. Each replicate was started

DOI: 10.1021/acs.jpcb.5b04822
J. Phys. Chem. B 2015, 119, 9696−9705

from six monomers at random positions, which were allowed to aggregate without constraints. The average maximum oligomerization state (i.e., monomer, dimer, etc.) as a function of simulated time is plotted in Figure 1a. The average aggregation rate for all systems studied are summarized in Table 3. Kassinin and neuromedin K aggregate considerably faster than $A\beta_{25-35}$. All simulations of tachykinin peptides reach the maximum hexamer state in around 100 ns, while some of the $A\beta_{25-35}$ simulations do not achieve the hexamer state even after 300 ns. As two of the $A\beta_{25-35}$ simulations reached only the tetramer state, we decided to test if this oligomerization state was particularly stable. To this end, we added further monomers to the final state at 300 ns and simulated the systems for another 100 ns. Enough monomers were added to reach a monomer concentration of 10 mM. Both simulations of $A\beta_{25-35}$ that had only reached the tetramer state continued to grow, showing that tetramers are not a uniquely stable state. However, tachykinin peptides still aggregate faster than $A\beta_{25-35}$ (see Figure S2). In particular, the oligomerization state of kassinin and neuromedin K increased on average by 5.8 and 5.0, respectively, while, the oligomerization state of $A\beta_{25-35}$ increased by only 3.2 during the 100 ns.

Table 3. Average Aggregation Rate for Each System Studied

system	NaCl (mM)	aggregation rate (monomer/ns)
$A\beta_{25-35}$	0	0.0138
kassinin	0	0.0519
neuromedin K	0	0.0475
$A\beta_{25-35}$ with capped C-terminus	0	0.0125
kassinin with uncapped C-terminus	0	0.0123
restrained $A\beta_{25-35}$	0	0.0085
kassinin in a β-hairpin	0	0.0173
$A\beta_{25-35}$	150	0.0108
kassinin	150	0.0157
neuromedin K	150	0.0147

Different properties were calculated for the aggregated hexamers. A summary of these properties are found in Table 4. All oligomers have a very low β-sheet content. Considering that β-sheets are characteristic of amyloid fibrils,[11] this suggests that longer simulations are needed to obtain fully formed β-sheet aggregates. Recent simulations combined with a transition network analysis have revealed that the initial aggregation leads to unordered oligomers, which subsequently reorder into β-sheets.[40] High β-sheet content was also observed in replica-exchange MD simulations of $A\beta_{25-35}$ with a coarse-grained model.[72] Therefore, one simulation per system was extended up to 1 μs. At the end of the simulations, a higher content of β-sheet is observed (12% for $A\beta_{25-35}$, 14% for kassinin and 13% for neuromedin K). Furthermore, the α-helix content remained minor in all cases. However, although it is still low, the α-helix content of neuromedin K is larger than that of kassinin and $A\beta_{25-35}$. This is an interesting observation because, while neuromedin K aggregates into fibrils, they have a higher α-helix content than normal amyloids as measured by circular dichroism.[12] It has been observed experimentally that when aggregated under different environmental conditions, oligomers with higher hydrophobic surface are more toxic.[73−76] Therefore, the average hydrophobic SASA was calculated. A correlation between amyloid toxicity and hydrophobic SASA was not observed. However, when normalized by the total SASA, a greater relative hydrophobic SASA is observed for $A\beta_{25-35}$ than for the tachykinin peptides. Neuromedin K and kassinin have relative hydrophobic SASAs of 0.52 ± 0.02 and 0.60 ± 0.02, respectively, which are lower than that of $A\beta_{25-35}$ which is 0.63 ± 0.01. By visual inspection, it was observed that some oligomers were much more extended than others. Thus, the asphericity was calculated as explained in the Methods section. Kassinin hexamers are the most aspherical, although it should be noted that standard deviations make all results from Table 4 almost indistinguishable. These quantities cannot be used to explain the difference in aggregation kinetics observed in Figure 1.

Influence of the C-Terminus. To understand how differences in primary structure generate such differences in aggregation kinetics, intermolecular contact maps including all oligomers were calculated for each peptide. These contact maps show the most probable contacts between residues of different monomers. Figure 2 shows the contact maps for $A\beta_{25-35}$, kassinin, and neuromedin K and example snapshots for the different oligomers. The most relevant interaction in $A\beta_{25-35}$ is between the C-terminus and the N-terminus of different monomers. This interaction is expected as $A\beta_{25-35}$ was simulated with uncapped termini, which means that the positively charged N-terminus can interact strongly with the negatively charged C-terminus. Moreover, there is a prominent hydrophobic interaction between the isoleucine residues at positions 7 and 8 of different monomers. The contact maps of the tachykinin peptides show that there is a substantial interaction between the C-termini of different monomers. In these peptides, the C-terminus is amidated, which allows for a strong interaction between the hydrophobic C-termini. This interaction is prohibited in $A\beta_{25-35}$ because of the negatively charged C-termini. In the case of neuromedin K, there is also a strong interaction between the hydrophobic cores (Phe^5-Phe^6-Val^7) of different monomers.

To confirm the importance of the C-terminal charge, the simulations were repeated with nonstandard termini. In particular, we simulated $A\beta_{25-35}$ with an amidated C-terminus and kassinin with a free acid C-terminus. The oligomerization state as a function of time are plotted in Figure 1b. For both proteins, aggregation is slower than in previous simulations. The contact maps for these simulations are plotted in Figure S3. As expected, for kassinin the interaction between the C-termini is diminished compared to the simulation with standard C-terminus and the interaction between the C- and N-terminus is augmented. In the case of $A\beta_{25-35}$, the interaction between C-termini becomes more relevant. These results suggest that the

Table 4. Summary of Properties of Aggregated Hexamers

peptide	hydrophobic SASA (nm^2)	relative hydrophobic SASA (%)	asphericity	β-sheet (%)	α-helix (%)
$A\beta_{25-35}$	31.2 ± 1.6	0.63 ± 0.01	0.18 ± 0.12	3.6 ± 0.2	0.19 ± 0.01
kassinin	34.9 ± 3.1	0.60 ± 0.02	0.26 ± 0.16	4.2 ± 0.2	0.14 ± 0.01
neuromedin K	26.3 ± 2.1	0.52 ± 0.02	0.14 ± 0.08	3.2 ± 0.2	1.72 ± 0.12

DOI: 10.1021/acs.jpcb.5b04822
J. Phys. Chem. B 2015, 119, 9696−9705

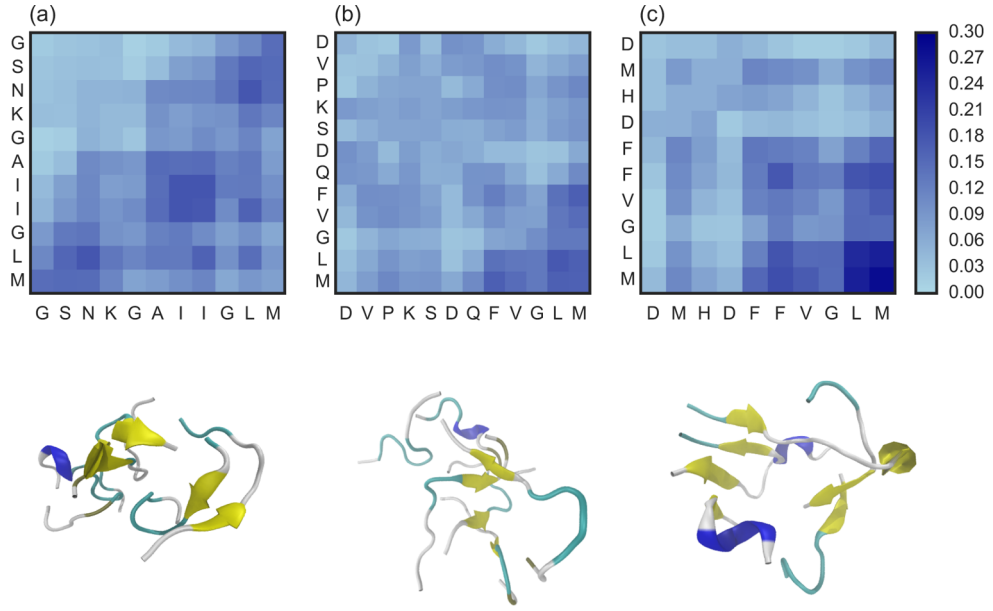

Figure 2. Intermolecular contact maps from the 300 ns simulations (above) and example snapshots from the extended 1 μs simulations (below) for the oligomers of (a) Aβ_{25-35}, (b) kassinin, and (c) neuromedin K.

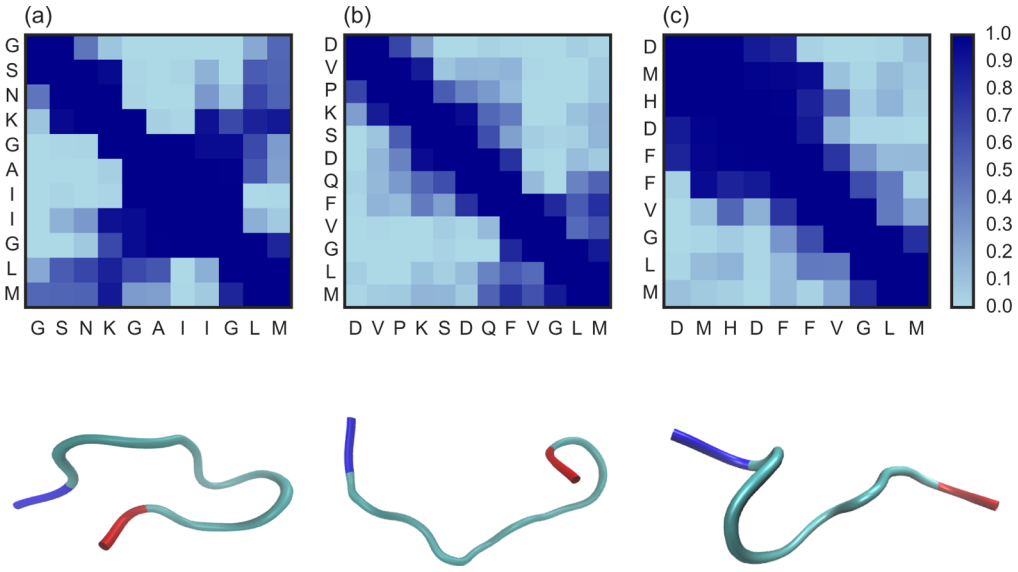

Figure 3. Intramolecular contact maps from the 50 ns simulations (above) and the most representative snapshot of the most probable cluster according to the clustering analysis (below) for the monomers of (a) Aβ_{25-35}, (b) kassinin, and (c) neuromedin K. The N-terminus is colored in blue and the C-terminus is colored in red.

charge of the C-terminus is essential to regulate the interaction between monomers in the aggregation of short amyloid peptides. However, it does not explain the difference in aggregation kinetics between the different peptides.

Monomer Conformations. To further understand why different peptides aggregate at different speeds, the behavior of the monomers before aggregation was studied. Figure 3 shows the intramolecular contact map for the different peptides and the most representative structures. The contact map defines the probability of an internal contact between different residues in a monomer. These contact maps show that Aβ_{25-35} is mostly in a hairpin-like conformation, as can be observed in the most probable structure and as was previously observed by Larini and Shea.[48] The structure is stabilized by a highly probable contact between Lys^4 and Met^{11}. This contact is caused by a salt bridge between the negatively charged C-terminus and the positive charge from the Lys^4 side-chain. Both kassinin and neuromedin K adopt a more extended conformation with no interaction between the two termini. In neuromedin K, a certain amount of helicity is found close to the N-terminus. To clarify these results, the secondary structure was calculated for the different peptides. In Figure 4, the probability of turn structure for each residue is plotted. The intermediate section of Aβ_{25-35} (Lys^4–Gly^5–Ala^6) has a turn content between 70% and 80%. Such a high turn content was not observed in the two tachykinin peptides.

These results lead us to hypothesize that a monomer in a hairpin-like conformation leads to slower aggregation kinetics. If this were true, we should observe that both Aβ_{25-35} and kassinin with nonstandard termini should also have a high

DOI: 10.1021/acs.jpcb.5b04822
J. Phys. Chem. B 2015, 119, 9696–9705

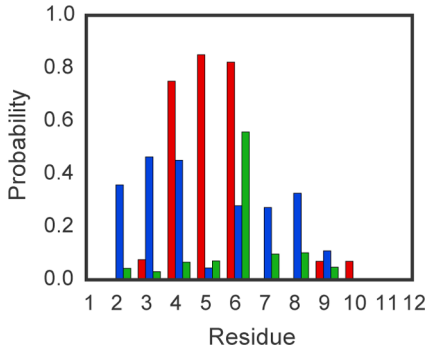

Figure 4. Probability of turn secondary structure per residue for the monomers of Aβ_{25-35} (red), kassinin (blue), and neuromedin K (green).

propensity for hairpin-like conformations. In Figure S4, the contact maps for the monomers of Aβ_{25-35} with amidated C-terminus and kassinin with charged C-terminus are plotted. In the case of Aβ_{25-35} with an amidated C-terminus, a hairpin-like conformation is still observed due to a nonspecific interaction of Met[11] with the central section (residues Ser[2]−Ile[7]) of the peptide. In the case of kassinin with a charged C-terminus, there is a strong interaction between the negatively charged C-terminus and Lys[4], which also leads to a hairpin-like structure. These structures, however, are not as likely as in Aβ_{25-35} with a charged C-terminus. A hairpin-like conformation has also been observed by Haspel et al.[77] in a simulation of neuromedin K with charged termini.

To further test the influence of monomer conformation on the aggregation kinetics, the simulation of Aβ_{25-35} was repeated with a restraint that stabilizes a hairpin-like conformation. This restraint forces the negatively charged C-terminus and Lys[4] to be close, limiting the flexibility of the peptides. The oligomerization state as a function of time for this system can be observed in Figure 1a. The aggregation kinetics decreases considerably compared to the unrestrained simulation, confirming that the monomer conformation influences the aggregation kinetics.

Considering the importance of the monomer conformation on the resulting aggregation kinetics, we decided to extend the 50 ns monomer simulations to 1 μs to better characterize the free energy surface of the monomer. For Aβ_{25-35} and neuromedin K, the conformation of the monomer did not change much (see Figure S5). However, while kassinin was mostly disordered during the first 50 ns, it turned into a β-hairpin during the 1 μs simulation (see Figure 5c and Figure S5). To test if this change in monomer conformation had an effect on aggregation kinetics, we repeated the aggregation simulations but starting from random monomer conformations from the last 800 ns of the 1 μs. The aggregation is slower, as can be observed in Figure 5a, but it is still faster than for Aβ_{25-35}. The contact map for the oligomers is plotted in Figure 5b. The contacts between the C-termini between different monomers are depleted in comparison to our initial simulation (Figure 2b). This confirms that the aggregation kinetics depends on the monomer conformation. In particular, it appears that the termini are important for contacts between different monomers and when they contact intramolecularly they are not available for the intermolecular contacts that drive aggregation.

Influence of Salt Concentration. It has been observed experimentally that the aggregation of amyloids depends strongly on environmental conditions such as pH or salt concentration.[29,31,78−80] To study the influence of salt concentration, we repeated the simulations for Aβ_{25-35} and the tachykinin peptides with a NaCl concentration of 150 mM. Figure 1c shows the aggregation of the three peptides at high salt concentration. The aggregation speed of tachykinin peptides is slower at high salt concentration than at low salt concentration, while the aggregation speed of Aβ_{25-35} is similar at both high and low salt concentrations. The difference in the effect of salt concentration on tachykinin peptides and Aβ_{25-35} signifies that the aggregation kinetics of the three peptides are more similar at high salt concentration than at low salt concentration. However, tachykinin peptides still aggregate slightly faster than Aβ_{25-35}. Figures S6 and S7 show the contact maps for the oligomers and monomers for these simulations. The most relevant intermolecular contacts are similar to those at low salt concentration, while monomers are mostly in a hairpin-like conformations, particularly for Aβ_{25-35} and kassinin. This may explain the reduced aggregation speed for the tachykinin peptides in the presence of 150 mM NaCl. Nonetheless, the results for the aggregation of the different amyloid peptides is surprising, as normally it is observed that amyloid aggregation is faster at higher salt concentration.[29,30] On the other hand, our simulations correlate with the experimental results of Naldi et al.,[20] who found that the aggregation of Aβ_{25-35} does not depend on salt concentration. These results also show the importance of simulating protein aggregation at the correct salt concentration.

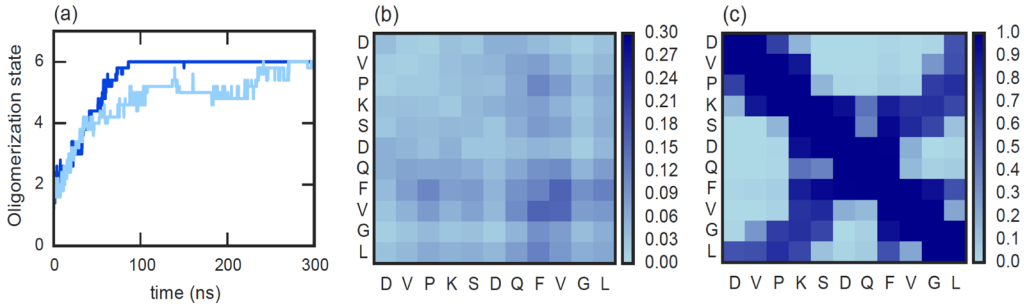

Figure 5. Aggregation of kassinin starting from a β-hairpin conformation. (a) Comparison between aggregation starting from an extended conformation (dark blue) and from a β-hairpin conformation (light blue). (b) Intermolecular contact map for the oligomers and (c) intramolecular contact map for the 1 μs monomer simulation.

DOI: 10.1021/acs.jpcb.5b04822
J. Phys. Chem. B 2015, 119, 9696−9705

DISCUSSION

Amyloids have been commonly associated with diseases such as Alzheimer's disease, Parkinson's disease, and type II diabetes. In this context, the discovery of functional amyloids has changed our understanding of the amyloid fold.[1,11] Because of their normal physiological role, functional amyloids must have evolved to lower their toxicity. Thus, considering that it is still unclear why aberrant amyloids are toxic, understanding the difference between functional and aberrant amyloids can help us treat amyloid-related diseases, and take advantage of functional amyloids for technological applications.[81] At the moment, there is strong evidence for soluble oligomers to be the toxic species in amyloid diseases.[3−6] Thus, peptides with stable oligomers should be the most toxic. If oligomers are thermodynamically unstable they have a higher chance of being degraded and avoid toxicity. However, if oligomers aggregate rapidly into fibrils, they would also be nontoxic. In this paper, we studied by means of MD simulations the aggregation of tachykinin peptides, which are known to form nontoxic functional amyloids,[15] and Alzheimer's Aβ_{25-35}. Our simulations suggest that tachykinin peptides may aggregate faster than the toxic Aβ_{25-35}. Even though this has not been studied experimentally for tachykinin peptides, it has been observed for other functional amyloids such as Pmel17, which aggregates faster than both Alzheimer's Aβ and Parkinson's α-synuclein.[13] These results suggest that some functional amyloids may avoid toxicity by aggregating rapidly into the nontoxic fibril phase.

Our simulations also suggest that the aggregation kinetics of tachykinin peptides and Aβ_{25-35} depend strongly on the charge of the C-terminus. C-terminal amidation is a common modification of proteins and can be essential for their function.[82] Particularly, C-terminal amidation is essential for tachykinin agonist activity.[83] Our simulations suggest that C-terminal amidation may be essential for the correct rapid aggregation of tachykinin peptides. It would be interesting to study experimentally if there is a difference in aggregation when uncapping tachykinin peptides. The effect of mutating neutral terminal residues to charged residues has been studied experimentally. It was found that changing the peptide STVIIE to STVIKT abolishes amyloid formation.[84] This result supports our finding that the aggregation speed of kassinin decreases when the C-terminus is not capped.

Another important observation from our simulations is that the conformation of the monomeric peptides could be useful in understanding aggregation kinetics. When monomeric peptides are in a hairpin-like conformation in which the two termini are close, then the peptide tends to aggregate more slowly. The reason for this could be that, in a hairpin-like conformation, termini interact intramolecularly and are not free to interact with other monomers. It is hard to predict how extensible these results are for larger peptides or proteins. Short peptides, such as the ones studied in this work, have much simpler internal dynamics, as they can only have a handful of stable monomer conformation, while larger peptides such as full-length Aβ can potentially have many different conformations. Thus, the simple model presented in this work likely cannot explain the aggregation kinetics of such large peptides or proteins. It should be noted, though, that when residues 17−36 of Alzheimer's Aβ_{40} are stabilized in a β-hairpin conformation, aggregation is inhibited.[85] Moreover, it has been observed that mutations that increase the toxicity of Aβ lead to monomer conformations with higher β-hairpin content.[86,87] Finally, it has been shown that short sections of a protein drive the aggregation of the entire protein,[84] which means that our conclusions could have general validity.

It should be emphasized that the results obtained in this paper are based on MD simulations and thus the limitations of such an approach should be taken into account. The two most important constraints of MD simulations are (a) lack of enough sampling and, (b) errors in the force field used. Limited computing power means that the entire aggregation free energy surface cannot be sampled. In our case, we limited ourselves to perform five independent 300 ns simulations for each system. Moreover, the systems are studied at a concentration of around 10 mM; a concentration at least an order of magnitude higher than the experimental value for tachykinin peptides.[15] Thus, monomers have many more collisions than experimentally observed and this could be an explanation for the fact that we do not observe large β-sheet content for the initial oligomers, contrary to what is observed experimentally for Aβ_{25-35}.[23] Regarding force fields, it has been observed that protein force fields overstabilize protein−protein interactions.[88] Considering these limitations, one should be cautious when interpreting these results. However, MD simulations are a relevant tool to understand molecular details and to propose new experiments. Based on the simulations in this paper, we hypothesize that the charge of the C-terminus can help to modulate the aggregation of tachykinin peptides, which would be interesting to investigate experimentally. Furthermore, we observe that the conformation of the monomeric peptide could be used to predict the aggregation kinetics. More evidence is needed, particularly for peptides for which the aggregation kinetics have been studied experimentally, to put this hypothesis on firmer ground.

CONCLUSIONS

Amyloid fibrils are related to diseases, including Alzheimer's disease, and functional roles such as hormone storage. In this study, we performed MD simulations of the aggregation of tachykinin peptides, which form functional amyloids, and Alzheimer's Aβ_{25-35}. We have observed differences in the aggregation process of these peptides. In particular, tachykinin peptides aggregate faster than Aβ_{25-35}. We also found that the charge of the C-terminus is essential in modulating the aggregation of these peptides. Furthermore, we observe that when monomeric peptides are in an extended conformation they tend to aggregate faster than when in a hairpin-like conformation. This suggests that when the interactions sites at the termini are free to interact, monomers aggregate faster. However, when the interaction sites have intramolecular contacts they are not free to drive aggregation.

ASSOCIATED CONTENT

Supporting Information

Comparison of the aggregation of neuromedin K with protonated and unprotonated His[3], results of the extension of the simulations of Aβ_{25-35}, kassinin and neuromedin K with a NaCl concentration of 0 mM, after adding 10 mM of nonaggregated monomers, intra- and intermolecular contact maps for simulations with unconventional C-termini and simulations with a NaCl concentration of 150 mM, and intramolecular contact maps for the 1 μs monomer simulations with a NaCl concentration of 0 mM. The Supporting Information is available free of charge on the ACS Publications website at DOI: 10.1021/acs.jpcb.5b04822.

DOI: 10.1021/acs.jpcb.5b04822
J. Phys. Chem. B 2015, 119, 9696−9705

AUTHOR INFORMATION

Corresponding Author

*E-mail: b.strodel@fz-juelich.de.

Notes

The authors declare no competing financial interest.

ACKNOWLEDGMENTS

We thank Bogdan Barz, Michael Owen and Oliver Schillinger for many insightful discussions. The authors gratefully acknowledge the computing time granted by the JARA-HPC Vergabegremium and provided on the JARA-HPC partition part of the RWTH Bull Cluster in Aachen (Grant Numbers JARA0018 and JARA0095). Financial support from the Deutsche Forschungsgemeinschaft (German Research Foundation, DFG) through Grant No. GSC 111 is acknowledged.

REFERENCES

(1) Chiti, F.; Dobson, C. M. Protein Misfolding, Functional Amyloid, and Human Disease. *Annu. Rev. Biochem.* **2006**, *75*, 333−366.

(2) Shewmaker, F.; McGlinchey, R. P.; Wickner, R. B. Structural Insights into Functional and Pathological Amyloid. *J. Biol. Chem.* **2011**, *286*, 16533−16540.

(3) Klein, W.; Stine, W.; Teplow, D. Small Assemblies of Unmodified Amyloid β-Protein Are the Proximate Neurotoxin in Alzheimer's Disease. *Neurobiol. Aging* **2004**, *25*, 569−580.

(4) Stefani, M. Biochemical and Biophysical Features of Both Oligomer/Fibril and Cell Membrane in Amyloid Cytotoxicity. *FEBS J.* **2010**, *277*, 4602−4613.

(5) Hayden, E.; Teplow, D. Amyloid β-Protein Oligomers and Alzheimer's Disease. *Alzheimer's Res. Ther.* **2013**, *5*, 60.

(6) Fändrich, M. Oligomeric Intermediates in Amyloid Formation: Structure Determination and Mechanisms of Toxicity. *J. Mol. Biol.* **2012**, *421*, 427−440.

(7) Lashuel, H. A.; Hartley, D.; Petre, B. M.; Walz, T.; Lansbury, P. T. Neurodegenerative Disease: Amyloid Pores from Pathogenic Mutations. *Nature* **2002**, *418*, 291.

(8) Glabe, C. G. Common Mechanisms of Amyloid Oligomer Pathogenesis in Degenerative Disease. *Neurobiol. Aging* **2006**, *27*, 570−575.

(9) Nasica-Labouze, J.; Nguyen, P. H.; Sterpone, F.; Berthoumieu, O.; Buchete, N.-V.; Coté, S.; De Simone, A.; Doig, A. J.; Faller, P.; Garcia, A.; et al. Amyloid β Protein and Alzheimer's Disease: When Computer Simulations Complement Experimental Studies. *Chem. Rev.* **2015**, *115*, 3518−3563.

(10) Fowler, D. M.; Koulov, A. V.; Balch, W. E.; Kelly, J. W. Functional Amyloid - from Bacteria to Humans. *Trends Biochem. Sci.* **2007**, *32*, 217−224.

(11) Greenwald, J.; Riek, R. Biology of Amyloid: Structure, Function, and Regulation. *Structure* **2010**, *18*, 1244−1260.

(12) Maji, S. K.; Perrin, M. H.; Sawaya, M. R.; Jessberger, S.; Vadodaria, K.; Rissman, R. A.; Singru, P. S.; Nilsson, K. P. R.; Simon, R.; Schubert, D.; et al. Functional Amyloids As Natural Storage of Peptide Hormones in Pituitary Secretory Granules. *Science* **2009**, *325*, 328−332.

(13) Fowler, D. M.; Koulov, A. V.; Alory-Jost, C.; Marks, M. S.; Balch, W. E.; Kelly, J. W. Functional Amyloid Formation Within Mammalian Tissue. *PLoS Biol.* **2006**, *4*, e6.

(14) Li, J.; McQuade, T.; Siemer, A. B.; Napetschnig, J.; Moriwaki, K.; Hsiao, Y.-S.; Damko, E.; Moquin, D.; Walz, T.; McDermott, A.; et al. The RIP1/RIP3 Necrosome Forms a Functional Amyloid Signaling Complex Required for Programmed Necrosis. *Cell* **2012**, *150*, 339−350.

(15) Singh, P. K.; Maji, S. K. Amyloid-like Fibril Formation by Tachykinin Neuropeptides and Its Relevance to Amyloid β-Protein Aggregation and Toxicity. *Cell Biochem. Biophys.* **2012**, *64*, 29−44.

(16) Maggio, J. E. Tachykinins. *Annu. Rev. Neurosci.* **1988**, *11*, 13−28.

(17) Flashner, E.; Raviv, U.; Friedler, A. The Effect of Tachykinin Neuropeptides on Amyloid β Aggregation. *Biochem. Biophys. Res. Commun.* **2011**, *407*, 13−17.

(18) Pieri, M.; Amadoro, G.; Carunchio, I.; Ciotti, M.; Quaresima, S.; Florenzano, F.; Calissano, P.; Possenti, R.; Zona, C.; Severini, C. SP Protects Cerebellar Granule Cells Against β-Amyloid-Induced Apoptosis by Down-Regulation and Reduced Activity of Kv4 Potassium Channels. *Neuropharmacology* **2010**, *58*, 268−276.

(19) Pike, C. J.; Walencewicz-Wasserman, A. J.; Kosmoski, J.; Cribbs, D. H.; Glabe, C. G.; Cotman, C. W. Structure-Activity Analyses of β-Amyloid Peptides: Contributions of the β25−35 Region to Aggregation and Neurotoxicity. *J. Neurochem.* **1995**, *64*, 253−265.

(20) Naldi, M.; Fiori, J.; Pistolozzi, M.; Drake, A. F.; Bertucci, C.; Wu, R.; Mlynarczyk, K.; Filipek, S.; de Simone, A.; Andrisano, V. Amyloid β-Peptide 25−35 Self-Assembly and Its Inhibition: A Model Undecapeptide System to Gain Atomistic and Secondary Structure Details of the Alzheimer's Disease Process and Treatment. *ACS Chem. Neurosci.* **2012**, *3*, 952−962.

(21) Yankner, B.; Duffy, L.; Kirschner, D. Neurotrophic and Neurotoxic Effects of Amyloid β Protein: Reversal by Tachykinin Neuropeptides. *Science* **1990**, *250*, 279−282.

(22) Shearman, M. Cellular MTT Reduction Distinguishes the Mechanism of Action of β-Amyloid from That of Tachykinin Receptor Peptides. *Neuropeptides* **1996**, *30*, 125−132.

(23) Bleiholder, C.; Do, T. D.; Wu, C.; Economou, N. J.; Bernstein, S. S.; Buratto, S. K.; Shea, J.-E.; Bowers, M. T. Ion Mobility Spectrometry Reveals the Mechanism of Amyloid Formation of Aβ(25−35) and Its Modulation by Inhibitors at the Molecular Level: Epigallocatechin Gallate and Scyllo-Inositol. *J. Am. Chem. Soc.* **2013**, *135*, 16926−16937.

(24) D'Ursi, A. M.; Armenante, M. R.; Guerrini, R.; Salvadori, S.; Sorrentino, G.; Picone, D. Solution Structure of Amyloid β-Peptide (25−35) in Different Media. *J. Med. Chem.* **2004**, *47*, 4231−4238.

(25) DuBay, K. F.; Pawar, A. P.; Chiti, F.; Zurdo, J.; Dobson, C. M.; Vendruscolo, M. Prediction of the Absolute Aggregation Rates of Amyloidogenic Polypeptide Chains. *J. Mol. Biol.* **2004**, *341*, 1317−1326.

(26) Pawar, A. P.; DuBay, K. F.; Zurdo, J.; Chiti, F.; Vendruscolo, M.; Dobson, C. M. Prediction of "Aggregation-Prone" and "Aggregation-Susceptible" Regions in Proteins Associated with Neurodegenerative Diseases. *J. Mol. Biol.* **2005**, *350*, 379−392.

(27) Xu, W.; Zhang, C.; Morozova-Roche, L.; Zhang, J. Z. H.; Mu, Y. pH-Dependent Conformational Ensemble and Polymorphism of Amyloid-β Core Fragment. *J. Phys. Chem. B* **2013**, *117*, 8392−8399.

(28) Kusumoto, Y.; Lomakin, A.; Teplow, D. B.; Benedek, G. B. Temperature Dependence of Amyloid β -Protein Fibrillization. *Proc. Natl. Acad. Sci. U. S. A.* **1998**, *95*, 12277−12282.

(29) Klement, K.; Wieligmann, K.; Meinhardt, J.; Hortschansky, P.; Richter, W.; Fändrich, M. Effect of Different Salt Ions on the Propensity of Aggregation and on the Structure of Alzheimer's Aβ(1−40) Amyloid Fibrils. *J. Mol. Biol.* **2007**, *373*, 1321−1333.

(30) Campioni, S.; Mannini, B.; López-Alonso, J. P.; Shalova, I. N.; Penco, A.; Mulvihill, E.; Laurents, D. V.; Relini, A.; Chiti, F. Salt Anions Promote the Conversion of HypF-N into Amyloid-like Oligomers and Modulate the Structure of the Oligomers and the Monomeric Precursor State. *J. Mol. Biol.* **2012**, *424*, 132−149.

(31) Buell, A. K.; Hung, P.; Salvatella, X.; Welland, M. E.; Dobson, C. M.; Knowles, T. P. Electrostatic Effects in Filamentous Protein Aggregation. *Biophys. J.* **2013**, *104*, 1116−1126.

(32) Chatani, E.; Naiki, H.; Goto, Y. Seeding-Dependent Propagation and Maturation of β_2-Microglobulin Amyloid Fibrils Under High Pressure. *J. Mol. Biol.* **2006**, *359*, 1086−1096.

(33) Breydo, L.; Reddy, K. D.; Piai, A.; Felli, I. C.; Pierattelli, R.; Uversky, V. N. The Crowd You're in With: Effects of Different Types of Crowding Agents on Protein Aggregation. *Biochim. Biophys. Acta, Proteins Proteomics* **2014**, *1844*, 346−357.

(34) Straub, J. E.; Thirumalai, D. Principles Governing Oligomer Formation in Amyloidogenic Peptides. *Curr. Opin. Struct. Biol.* **2010**, *20*, 187−195.

DOI: 10.1021/acs.jpcb.5b04822
J. Phys. Chem. B 2015, 119, 9696−9705

(35) Straub, J. E.; Thirumalai, D. Toward a Molecular Theory of Early and Late Events in Monomer to Amyloid Fibril Formation. *Annu. Rev. Phys. Chem.* **2011**, *62*, 437−463.
(36) Dror, R. O.; Dirks, R. M.; Grossman, J.; Xu, H.; Shaw, D. E. Biomolecular Simulation: A Computational Microscope for Molecular Biology. *Annu. Rev. Biophys.* **2012**, *41*, 429−452.
(37) Nguyen, P.; Derreumaux, P. Understanding Amyloid Fibril Nucleation and Aβ Oligomer/Drug Interactions from Computer Simulations. *Acc. Chem. Res.* **2014**, *47*, 603−611.
(38) Gsponer, J.; Haberthür, U.; Caflisch, A. The Role of Side-Chain Interactions in the Early Steps of Aggregation: Molecular Dynamics Simulations of an Amyloid-Forming Peptide from the Yeast Prion Sup35. *Proc. Natl. Acad. Sci. U. S. A.* **2003**, *100*, 5154−5159.
(39) Reddy, G.; Straub, J. E.; Thirumalai, D. Dynamics of Locking of Peptides onto Growing Amyloid Fibrils. *Proc. Natl. Acad. Sci. U. S. A.* **2009**, *106*, 11948−11953.
(40) Barz, B.; Wales, D. J.; Strodel, B. A Kinetic Approach to the Sequence-Aggregation Relationship in Disease-Related Protein Assembly. *J. Phys. Chem. B* **2014**, *118*, 1003−1011.
(41) De Simone, A.; Derreumaux, P. Low Molecular Weight Oligomers of Amyloid Peptides Display β-Barrel Conformations: A Replica Exchange Molecular Dynamics Study in Explicit Solvent. *J. Chem. Phys.* **2010**, *132*, 165103.
(42) Dupuis, N. F.; Wu, C.; Shea, J.-E.; Bowers, M. T. The Amyloid Formation Mechanism in Human IAPP: Dimers Have β-Strand Monomer-Monomer Interfaces. *J. Am. Chem. Soc.* **2011**, *133*, 7240−7243.
(43) Matthes, D.; Gapsys, V.; Daebel, V.; de Groot, B. L. Mapping the Conformational Dynamics and Pathways of Spontaneous Steric Zipper Peptide Oligomerization. *PLoS One* **2011**, *6*, e19129.
(44) Matthes, D.; Gapsys, V.; de Groot, B. L. Driving Forces and Structural Determinants of Steric Zipper Peptide Oligomer Formation Elucidated by Atomistic Simulations. *J. Mol. Biol.* **2012**, *421*, 390−416.
(45) Matthes, D.; Daebel, V.; Meyenberg, K.; Riedel, D.; Heim, G.; Diederichsen, U.; Lange, A.; de Groot, B. L. Spontaneous Aggregation of the Insulin-Derived Steric Zipper Peptide VEALYL Results in Different Aggregation Forms with Common Features. *J. Mol. Biol.* **2014**, *426*, 362−376.
(46) Wei, G.; Jewett, A. I.; Shea, J.-E. Structural Diversity of Dimers of the Alzheimer Amyloid-β(25−35) Peptide and Polymorphism of the Resulting Fibrils. *Phys. Chem. Chem. Phys.* **2010**, *12*, 3622−3629.
(47) Riccardi, L.; Nguyen, P. H.; Stock, G. Construction of the Free Energy Landscape of Peptide Aggregation from Molecular Dynamics Simulations. *J. Chem. Theory Comput.* **2012**, *8*, 1471−1479.
(48) Larini, L.; Shea, J.-E. Role of β-Hairpin Formation in Aggregation: The Self-Assembly of the Amyloid-β(25−35) Peptide. *Biophys. J.* **2012**, *103*, 576−586.
(49) Nguyen, P. H.; Li, M. S.; Derreumaux, P. Effects of All-Atom Force Fields on Amyloid Oligomerization: Replica Exchange Molecular Dynamics Simulations of the Aβ_{16-22} Dimer and Trimer. *Phys. Chem. Chem. Phys.* **2011**, *13*, 9778−9788.
(50) Nguyen, P. H.; Derreumaux, P. Conformational Ensemble and Polymorphism of the All-Atom Alzheimer's Aβ_{37-42} Amyloid Peptide Oligomers. *J. Phys. Chem. B* **2013**, *117*, 5831−5840.
(51) Barz, B.; Olubiyi, O. O.; Strodel, B. Early Amyloid β-Protein Aggregation Precedes Conformational Change. *Chem. Commun.* **2014**, *50*, 5373−5375.
(52) Hess, B.; Kutzner, C.; van der Spoel, D.; Lindahl, E. GROMACS 4: Algorithms for Highly Efficient, Load-Balanced, and Scalable Molecular Simulation. *J. Chem. Theory Comput.* **2008**, *4*, 435−447.
(53) Jorgensen, W. L.; Tirado-Rives, J. The OPLS Potential Functions for Proteins, Energy Minimizations for Crystals of Cyclic Peptides and Crambin. *J. Am. Chem. Soc.* **1988**, *110*, 1657−1666.
(54) Kaminski, G. A.; Friesner, R. A.; Tirado-Rives, J.; Jorgensen, W. L. Evaluation and Reparametrization of the OPLS-AA Force Field for Proteins Via Comparison with Accurate Quantum Chemical Calculations on Peptides. *J. Phys. Chem. B* **2001**, *105*, 6474−6487.
(55) Jorgensen, W. L.; Chandrasekhar, J.; Madura, J. D.; Impey, R. W.; Klein, M. L. Comparison of Simple Potential Functions for Simulating Liquid Water. *J. Chem. Phys.* **1983**, *79*, 926−935.
(56) Humphrey, W.; Dalke, A.; Schulten, K. VMD: Visual Molecular Dynamics. *J. Mol. Graphics* **1996**, *14*, 33−38.
(57) Grace, R. C. R.; Lynn, A. M.; Cowsik, S. M. Lipid Induced Conformation of the Tachykinin Peptide Kassinin. *J. Biomol. Struct. Dyn.* **2001**, *18*, 611−625.
(58) Mantha, A. K.; Chandrashekar, I. R.; Baquer, N. Z.; Cowsik, S. M. Three Dimensional Structure of Mammalian Tachykinin Peptide Neurokinin B Bound to Lipid Micelles. *J. Biomol. Struct. Dyn.* **2004**, *22*, 137−147.
(59) Darden, T.; York, D.; Pedersen, L. Particle Mesh Ewald: An $N\cdot\log(N)$ Method for Ewald Sums in Large Systems. *J. Chem. Phys.* **1993**, *98*, 10089−10092.
(60) Hess, B. P-LINCS: A Parallel Linear Constraint Solver for Molecular Simulation. *J. Chem. Theory Comput.* **2008**, *4*, 116−122.
(61) Miyamoto, S.; Kollman, P. A. Settle: An Analytical Version of the SHAKE and RATTLE Algorithm for Rigid Water Models. *J. Comput. Chem.* **1992**, *13*, 952−962.
(62) Feenstra, K. A.; Hess, B.; Berendsen, H. J. C. Improving Efficiency of Large Time-Scale Molecular Dynamics Simulations of Hydrogen-Rich Systems. *J. Comput. Chem.* **1999**, *20*, 786−798.
(63) Parrinello, M.; Rahman, A. Polymorphic Transitions in Single Crystals: A New Molecular Dynamics Method. *J. Appl. Phys.* **1981**, *52*, 7182−7190.
(64) Nosé, S.; Klein, M. Constant Pressure Molecular Dynamics for Molecular Systems. *Mol. Phys.* **1983**, *50*, 1055−1076.
(65) Nosé, S. A. Unified Formulation of the Constant Temperature Molecular Dynamics Methods. *J. Chem. Phys.* **1984**, *81*, 511−519.
(66) Hoover, W. G. Canonical Dynamics: Equilibrium Phase-Space Distributions. *Phys. Rev. A: At., Mol., Opt. Phys.* **1985**, *31*, 1695−1697.
(67) Michaud-Agrawal, N.; Denning, E. J.; Woolf, T. B.; Beckstein, O. MDAnalysis: A Toolkit for the Analysis of Molecular Dynamics Simulations. *J. Comput. Chem.* **2011**, *32*, 2319−2327.
(68) Eisenhaber, F.; Lijnzaad, P.; Argos, P.; Sander, C.; Scharf, M. The Double Cubic Lattice Method: Efficient Approaches to Numerical Integration of Surface Area and Volume and to Dot Surface Contouring of Molecular Assemblies. *J. Comput. Chem.* **1995**, *16*, 273−284.
(69) Kabsch, W.; Sander, C. Dictionary of Protein Secondary Structure: Pattern Recognition of Hydrogen-Bonded and Geometrical Features. *Biopolymers* **1983**, *22*, 2577−2637.
(70) Dima, R. I.; Thirumalai, D. Asymmetry in the Shapes of Folded and Denatured States of Proteins. *J. Phys. Chem. B* **2004**, *108*, 6564−6570.
(71) Daura, X.; Gademann, K.; Jaun, B.; Seebach, D.; van Gunsteren, W. F.; Mark, A. E. Peptide Folding: When Simulation Meets Experiment. *Angew. Chem., Int. Ed.* **1999**, *38*, 236−240.
(72) Spill, Y. G.; Pasquali, S.; Derreumaux, P. Impact of Thermostats on Folding and Aggregation Properties of Peptides Using the Optimized Potential for Efficient Structure Prediction Coarse-Grained Model. *J. Chem. Theory Comput.* **2011**, *7*, 1502−1510.
(73) Campioni, S.; Mannini, B.; Zampagni, M.; Pensalfini, A.; Parrini, C.; Evangelisti, E.; Relini, A.; Stefani, M.; Dobson, C. M.; Cecchi, C.; et al. A Causative Link Between the Structure of Aberrant Protein Oligomers and Their Toxicity. *Nat. Chem. Biol.* **2010**, *6*, 140−147.
(74) Bolognesi, B.; Kumita, J. R.; Barros, T. P.; Esbjorner, E. K.; Luheshi, L. M.; Crowther, D. C.; Wilson, M. R.; Dobson, C. M.; Favrin, G.; Yerbury, J. J. ANS Binding Reveals Common Features of Cytotoxic Amyloid Species. *ACS Chem. Biol.* **2010**, *5*, 735−740.
(75) Krishnan, R.; Goodman, J. L.; Mukhopadhyay, S.; Pacheco, C. D.; Lemke, E. A.; Deniz, A. A.; Lindquist, S. Conserved Features of Intermediates in Amyloid Assembly Determine Their Benign or Toxic States. *Proc. Natl. Acad. Sci. U. S. A.* **2012**, *109*, 11172.
(76) Ladiwala, A. R. A.; Litt, J.; Kane, R. S.; Aucoin, D. S.; Smith, S. O.; Ranjan, S.; Davis, J.; van Nostrand, W. E.; Tessier, P. M. Conformational Differences Between Two Amyloid β Oligomers of

DOI: 10.1021/acs.jpcb.5b04822
J. Phys. Chem. B 2015, 119, 9696−9705

Similar Size and Dissimilar Toxicity. *J. Biol. Chem.* **2012**, *287*, 24765−24773.
(77) Haspel, N.; Laurent, A. D.; Zanuy, D.; Nussinov, R.; Alemán, C.; Puiggalí, J.; Revilla-López, G. Conformational Exploration of Two Peptides and Their Hybrid Polymer Conjugates: Potentialities As Self-Aggregating Materials. *J. Phys. Chem. B* **2012**, *116*, 13941−13952.
(78) Hoyer, W.; Antony, T.; Cherny, D.; Heim, G.; Jovin, T. M.; Subramaniam, V. Dependence of α-Synuclein Aggregate Morphology on Solution Conditions. *J. Mol. Biol.* **2002**, *322*, 383−393.
(79) Petkova, A.; Buntkowsky, G.; Dyda, F.; Leapman, R.; Yau, W.-M.; Tycko, R. Solid State NMR Reveals a pH-Dependent Antiparallel β-Sheet Registry in Fibrils Formed by a β-Amyloid Peptide. *J. Mol. Biol.* **2004**, *335*, 247−260.
(80) Castelletto, V.; Hamley, I.; Cenker, C.; Olsson, U. Influence of Salt on the Self-Assembly of Two Model Amyloid Heptapeptides. *J. Phys. Chem. B* **2010**, *114*, 8002−8008.
(81) Knowles, T. P. J.; Buehler, M. J. Nanomechanics of Functional and Pathological Amyloid Materials. *Nat. Nanotechnol.* **2011**, *6*, 469−479.
(82) Merkler, D. J. C-Terminal Amidated Peptides: Production by the in vitro Enzymatic Amidation of Glycine-Extended Peptides and the Importance of the Amide to Bioactivity. *Enzyme Microb. Technol.* **1994**, *16*, 450−456.
(83) Patacchini, R.; Quartara, L.; Rovero, P.; Goso, C.; Maggi, C. A. Role of C-Terminal Amidation on the Biological Activity of Neurokinin A Derivatives with Agonist and Antagonist Properties. *J. Pharm. Exp. Ther.* **1993**, *264*, 17−21.
(84) Esteras-Chopo, A.; Serrano, L.; López de la Paz, M. The Amyloid Stretch Hypothesis Recruiting Proteins Toward the Dark Side. *Proc. Natl. Acad. Sci. U. S. A.* **2005**, *102*, 16672−16677.
(85) Hoyer, W.; Grönwall, C.; Jonsson, A.; Ståhl, S.; Härd, T. Stabilization of a β-Hairpin in Monomeric Alzheimer's Amyloid-β Peptide Inhibits Amyloid Formation. *Proc. Natl. Acad. Sci. U. S. A.* **2008**, *105*, 5099−5104.
(86) Nguyen, P. H.; Tarus, B.; Derreumaux, P. Familial Alzheimer A2 V Mutation Reduces the Intrinsic Disorder and Completely Changes the Free Energy Landscape of the Aβ1−28 Monomer. *J. Phys. Chem. B* **2014**, *118*, 501−510.
(87) Das, P.; Murray, B.; Belfort, G. Alzheimer's Protective A2T Mutation Changes the Conformational Landscape of the Aβ_{1-42} Monomer Differently Than Does the A2V Mutation. *Biophys. J.* **2015**, *108*, 738−747.
(88) Petrov, D.; Zagrovic, B. Are Current Atomistic Force Fields Accurate Enough to Study Proteins in Crowded Environments? *PLoS Comput. Biol.* **2014**, *10*, e1003638.

DOI: 10.1021/acs.jpcb.5b04822
J. Phys. Chem. B 2015, 119, 9696−9705